shRNA targeting Bmi-1 sensitizes CD44+ nasopharyngeal cancer stem-like cells to radiotherapy

XIN-HUA XU[1,2], XIAO-YAN LIU[1], JIN SU[2], DAO-JUN LI[2], QIAO HUANG[2], MING-QIAN LU[1], FANG YI[2], JING-HUA REN[3] and WEI-HONG CHEN[3]

[1]Department of Oncology, The First College of Clinical Medical Science, China Three Gorges University, Yichang Central People's Hospital, Yichang, Hubei; [2]Oncology Institute, China Three Gorges University, Yichang, Hubei; [3]Cancer Center, Union Hospital, Tongji Medical College, Huazhong University of Science and Technology, Wuhan, Hubei, P.R. China

Received March 2, 2014; Accepted May 12, 2014

DOI: 10.3892/or.2014.3267

Abstract. Accumulating evidence indicates that cancer stem cells (CSCs) are involved in resistance to radiation therapy (RT). Bmi-1, a member of the Polycomb family of transcriptional repressors, is essential for maintaining the self-renewal abilities of stem cells and overexpression of Bmi-1 correlates with cancer therapy failure. Our previous study identified that the CD44+ nasopharyngeal cancer (NPC) cells may be assumed as one of markers of nasopharyngeal carcinoma cancer stem cell-like cells (CSC-LCs) and Bmi-1 is overexpressed in CD44+ NPC. In the present study, we used RNA interference technology to knock down the expression of Bmi-1 in CD44+ NPC cells, and then measured the radiation response by clonogenic cell survival assay. DNA repair was monitored by γH2AX foci formation. Bmi-1 downstream relative gene and protein expression of p16, p14, p53 were assessed by western blotting and real-time PCR. Cell cycle and apoptosis were detected by flow cytometry assays. We found that Bmi-1 knockdown prolonged G1 and enhanced the radiation-induced G2/M arrest, inhibited DNA damage repair, elevated protein p16, p14 and p53 expression, leading to increased apoptosis in the radiated CD44+ cells. These data suggest that Bmi-1 downregulation increases the radiosensitivity to CD44+ NPC CSC-LCs. Bmi-1 is a potential target for increasing the sensitivity of NPC CSCs to radiotherapy.

Introduction

Nasopharyngeal cancer (NPC) is currently the most lethal head and neck neoplasm in Southeast Asia, especially in the Cantonese region, and radiotherapy is a cornerstone in the treatment of this malignancy. However, the efficacy of radiotherapy, particularly for advanced patients, is limited due to the development of radioresistance. Evidence has suggested that cancer stem cells (CSCs) are involved in resistance to various forms of therapies, including radiotherapy, and represent potentially useful pharmacologic targets (1-3). However, the interaction between radioresistance and CSCs and its underlying mechanisms have not been previously explored. B-cell-specific Moloney murine leukemia virus integration site 1 (Bmi-1), a member of the Polycomb family of transcriptional repressors, is essential for maintaining the self-renewal and differentiation of human stem cells (4-7). Bmi-1 has been demonstrated to be overexpressed in various of tumors (8), such as lung (9), breast (10) and prostate cancer (11), esophageal carcinoma (12) and NPC (13). Bmi-1 inhibition has been shown to sensitize those tumor cells to radiation (10,14,15). However, whether Bmi-1 inhibition can potentiate the cytotoxic effects of radiation on nasopharyngeal CSCs remains to be elucidated.

Our previous study identified that the CD44+ NPC cells, derived from the human NPC cell line SUNE-1 5-8F, with high capacity of self-renewal, differentiation abilities, tumorigenesis and radiochemoresistance, may be assumed to be one of the markers of nasopharyngeal carcinoma cancer stem cell-like cells (CSC-LCs) and Bmi-1 is overexpressed in CD44+ NPC (16). To further explore the functional role of Bmi-1 in NPC-CD44+ cells, we used a lentiviral vector expressing shRNA to knock down Bmi-1 expression (sh-Bmi-1) in NPC-CD44+ cells and evaluated the effects of Bmi-1 inhibition by shRNA on the sensitivity of NPC-CD44+ cells to radiation, DNA damage and repair, cell cycle distribution and apoptosis, and Bmi-1 downstream related protein for the purpose of improving the radiosensitivity of nasopharyngeal cancer stem-like cells, which may provide a broad potential therapeutic paradigm against NPC.

Materials and methods

Cell culture and reagents. The human NPC cell line SUNE-1 5-8F was purchased from Xiang-Ya Central Experiment

Correspondence to: Dr Xin-Hua Xu, Department of Oncology, The First College of Clinical Medical Science, China Three Gorges University, Yichang Central People's Hospital, 183 Yiling Road, Yichang, Hubei 443002, P.R. China
E-mail: xuxinhua@medmail.com.cn

Key words: Bmi-1, CD44+, cancer stem cell-like cells, nasopharyngeal carcinoma, radiosensitivity

Laboratory, and was maintained in RPMI-1640 medium supplemented with 10% fetal bovine serum in a humidified incubator (37˚C, 5% carbon dioxide). Purified CD44+ nasopharyngeal cancer stem-like cells were cultured in DMEM/F12 medium supplemented with 20 ng/ml EGF, 10 ng/ml bFGF, 5 μg/ml insulin and 0.4% bovine serum albumin (BSA).

Flow cytometric analysis and cell sorting (FACS). The cell sorting procedures were the same as previously described (16). After sorting, an aliquot of sorted cells was always reanalyzed to check for purity, which was generally >95%.

Generation of stable Bmi-1 knockdown (KD) cell lines. Sequence-specific oligonucleotide stretch shRNA designed to target the Bmi-1 (gene sequence no. NM_005180) were synthesized as follows: Bmi1-RNAi (19426-1), 5'-TAATACTT TCCAGATTGAT-3'; Bmi1-RNAi (19427-1), 5'-GAAAGTAA ACAAAGACAAA-3'; Bmi1-RNAi (19428-1), 5'-AGAACAG ATTGGATCGGAA-3'; loop sequence CTCGAG. Retroviral vector Bmi-1 short hairpin RNA (shRNA) was constructed by GeneChem (Shanghai, China). Bmi-1 gene was introduced into CD44+ NPC cells by infecting cells with a retroviral vector LV-BMI1-RNAi (19428-1) KD. Negative control cells (NC) were infected with the empty retroviral vector GV118-U6-MCS-Ubi-EGFP (GeneChem). The lentivirus stock [LV-BMI1-RNAi (19428-1)] was added to CD44+ cells at a multiplicity of infection (MOI) of 30. The cells without transfection were used as a blank control (CON). Transfection rates were monitored with fluorescence microscopy. The silencing of Bmi-1 was confirmed by western blotting and real-time PCR analysis.

Real-time PCR. Total RNA was isolated using TRIzol reagent (Invitrogen). Reverse transcription (RT) was performed using 1 μg of total RNA and the MML-V reverse transcriptase (Invitrogen). Real-time PCR was performed using the Platinum SYBR-Green Super Mix (Invitrogen) and a real-time PCR apparatus (ABI Prism 7000). Primer sets used were: Bmi-1 (F), 5'-CCACCTGATGTGTGTGCTTTG-3' and (R), 5'-TTCAGTAGTGGTCTGGTCTTGT-3'; p16 (F), 5'-GGAGT TTTCAGAAGGGGTTTGT-3' and (R), 5'-CCTCATTCCTCT TCCTTGGTTT-3'; p14 (F), 5'-TTCTGCCTTTTCACTGTGT TGGA-3' and (R), 5'-CTCAAGAGAAGCCAGTAACCC-3'; GAPDH (F), 5'-TGACTTCAACAGCGACACCCA-3' and (R), 5'-CACCCTGTTGCTGTAGCCAAA-3'; β-actin (F), 5'-GTCC ACCGCAAATGCTTCTA-3' and (R), 5'-TGCTGTCACCTTC ACCGTTC-3'. GAPDH and β-actin were used as internal standard for data calibration, which was for Bmi-1, and p16 and p14, respectively. The $2^{\Delta\Delta Ct}$ formula was used for the calculation of differential gene expression.

Western blot analysis. Cells were lysed in lysis buffer [25 mM Tris-HCl pH 7.5, 2.5 mM EDTA, 137 mM NaCl, 2.7 mM KCl, 1% sodium deoxycholic acid, 0.1% SDS, 1% Triton X-100, 2 mM PMSF and protease inhibitor cocktail (Nacalai Tesque)] for 30 min at 4˚C. Lysates were clarified by centrifugation at 12,000 rpm for 15 min at 4˚C, and the supernatants were collected. Protein concentrations were measured using a DC Protein Assay kit (Bio-Rad Laboratories, Hercules, CA, USA). An equal amount of the protein from each sample was separated by sodium dodecyl sulfate-polyacrylamide gel electrophoresis (SDS-PAGE) and transferred to a polyvinylidene difluoride (PVDF) membrane (Immobilon; Millipore). The membranes were developed using Immobilon Western Detection Reagents (Millipore) according to the manufacturer's instructions. The chemiluminescence of the membrane was detected using VersaDoc (Bio-Rad). Densitometric analyses of the band intensities were performed using ImageJ software (version 1.38x; National Institutes of Health). The following antibodies were used: Bmi-1 (1:1,000; rabbit anti-human); p16 (1:200; rabbit anti-human) (both from Epitomics); p14 (1:200; rabbit anti-human) and p53 (1:1,000; rabbit anti-human) (both from Cell Signaling Technology). β-actin protein levels were used as a control to verify equal protein loading.

Immunofluorescence staining. Cells were seeded on coverslips in 24-well plates and allowed to grow overnight. Cells were irradiated with a single dose of 2 Gy. Then, cells were washed and fixed with 4% paraformaldehyde at specific measuring times (0.5, 6, 12 and 24 h) and cells were rinsed in phosphate-buffered saline (PBS). After blocking in 5% BSA at room temperature for 30 min, slides were incubated with γH2AX antibody, mouse anti-human (Abcam) at 4˚C overnight and then incubated with goat anti-mouse IgG-conjugated with PE (Abbkine). Images were captured by Olympus laser scanning confocal microscopy (Olympus Optical Co., Tokyo, Honshu, Japan). Cells were judged as 'positive' for γH2AX foci when they displayed 10 or more discrete dots of brightness. For quantitation of foci, a minimum of 100 cells were analyzed for each time point. All data points represent means ± SD of three experiments.

Colony formation assay. The exponential growth cells were plated on six-well plates with 200-6,000 cells/well, irradiated the next day at the distinct doses (0, 2, 4, 6 and 8 Gy). The cells were maintained in culture for an additional 14 days to allow colony formation, then fixed with methanol, stained with 0.5% crystal violet (Sigma) and colonies containing at least 50 cells in size were counted. Each treatment was carried out in triplicate. Cell survival fraction (SF), radiation dose (D), the bottom of the natural logarithm (e), the mean death dose (D_0) and extrapolate number (N) were used for cell survival curves. Finally, the sensitization enhancing ratio (SER) was calculated (a ratio of SF_2).

Cell cycle analysis. The cells were harvested and fixed in 70% ethanol at 4˚C overnight. Next day, cells were suspended in 200 μl PBS and 2 μl RNase A (5 mg/ml). After 30 min incubation, 10 μl PI (1 mg/ml) was added and the cells were incubated for 30 min in the dark for analysis. The flow cytometry data was acquired using FACSCanto II flow cytometer (BD Biosciences, San Jose, CA, USA) and the results were analyzed by ModFit LT2.0 software (Coulter Electronics).

Cell apoptosis analysis. The cells were exposed to 6 Gy X-rays, 24 h after IR and cells were treated according to the Annexin V-PE/7-AAD apoptosis detection kit (KeyGen, Nanjing, Jiangsu, China). Cells were harvested and resuspended in 50 μl of binding buffer and 7-AAD (5 μl) in the dark for 10 min, at room temperature. Then, binding buffer

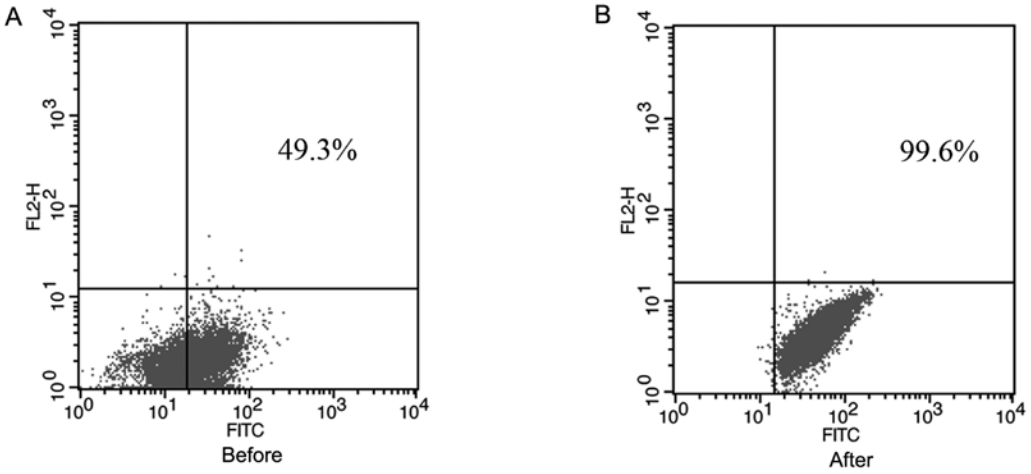

Figure 1. Cell sorting results and sorting purity. (A) In the NPC cell line, SUNE-1 5-8F, CD44$^+$ cells occupied ~49.3% of the total cells. (B) The sorting purity of the freshly sorted CD44$^+$ cells was 99.6%. NPC, nasopharyngeal cancer.

(450 μl) and 1 μl Annexin V-PE were added in the dark for 10 min, at room temperature, and cells were analyzed by flow cytometry. PE-positive cells were regarded as apoptotic cells. This experiment was repeated three times.

Statistical analysis. Results are expressed as the means ± SD. Analysis was performed using a two-way Student's t-test. $P<0.05$ was considered to indicate a statistically significant difference.

Results

FACS detects CD44 expression in the SUNE-1 5-8F cells, and the sorting purity. We examined CD44 expression in the human NPC SUNE-1 5-8F cell line by flow cytometry. As shown in Fig. 1, in the NPC cell line SUNE-1 5-8F, CD44$^+$ cells occupied ~49.3% of the total cells, which was in agreement with our previous study (43-52%) (16). CD44$^+$ cells were collected for subsequent experiments. The purity of these cells was 99.6%.

Knockdown of Bmi-1 by lentivirus-mediated RNA interference in CD44$^+$ NPC cells. Previous studies in other systems suggested that Bmi-1 expression was associated with significantly reduced patient survival (17-19) after RT with or without chemotherapy, indicating that Bmi-1 overexpression may be mediating radioresistance. To address this possibility, CD44$^+$ NPC-CLCs cells were transfected with lentivirus-mediated RNA targeting Bmi-1 [LV-BMI1-RNAi (19428-1), KD]. Control cells were infected with the empty retroviral vector GV118-U6-MCS-Ubi-EGFP, NC. To ensure the transfection efficiency of lentivirus into CD44$^+$ NPC CLCs cells, GFP expression was monitored by fluorescence microscopy and FACS analysis. It showed a high-efficiency infection that the majority of cells displayed green fluorescence 72 h after lentivirus transfection, with the efficiency reaching >90% in both KD and NC-treated cells (Fig. 2A). LV-Bmi-1-RNAi showed 90% reduction in Bmi-1 transcript level, observed at 72 h post-transfection by real-time PCR (Fig. 2B), which resulted in nearly undetectable Bmi-1 protein expression (Fig. 2C).

Table I. The main parameters of cell survival curves after ionizing radiation.[a]

Parameters	CON	NC	KD
D_0	2.89	2.83	2.14
D_q	3.36	2.42	0.34
N	2.16	1.85	1.16
SF_2	0.78	0.71	0.44
SER	1.10	1.77	

[a]Survival curves with surviving fractions (SFs) normalized to the plating efficiency were fitted according to multi-target click model: $SF = 1 - (1 - e^{-D/D_0})^N$. D_0, mean lethal dose; D_q, quasi-threshold dose; N, extrapolation number; SF_2, surviving fraction at 2 Gy; SER, radiation sensitizing enhancement ratio. SER=1 suggests an additive radiation effect and SER >1, a supra-additive effect as against a sub-additive effect in the case of SER <1. CON, control; NC, negative control; KD, knockdown.

Real-time PCR and western blot detection of the Bmi-1 downstream related genes p16, p14 and p53 mRNA and protein changes. Emerging evidence indicates that Bmi-1 is upregulated in various malignancies and promotes tumor progression by inhibiting the transcription of tumor suppressors, such as p53, $p16^{INK4a}$ and $p14^{Arf}$ (15,20-23). As shown in Fig. 3, knockdown of Bmi-1 increased the downstream related genes p16, p14 and p53 mRNA and protein levels.

Bmi-1 knockdown sensitizes CD44$^+$ NPC CLCs to radiation. To determine the radiosensitizing effect of Bmi-1 depletion on the CD44$^+$ NPC CLCs, a clonogenic formation assay was performed. As depicted in Fig. 4, the shoulder area of the survival curves was significantly narrowed and the surviving fractions (SFs) at each dose (2, 4, 6 and 8 Gy) decreased in Bmi-1-depleted cells. The values of SF_2, D_0, D_q and N were all lower in Bmi-1 KD cells (Table I). SF_2 was reduced to 44% in KD cells from 78% in CON cells

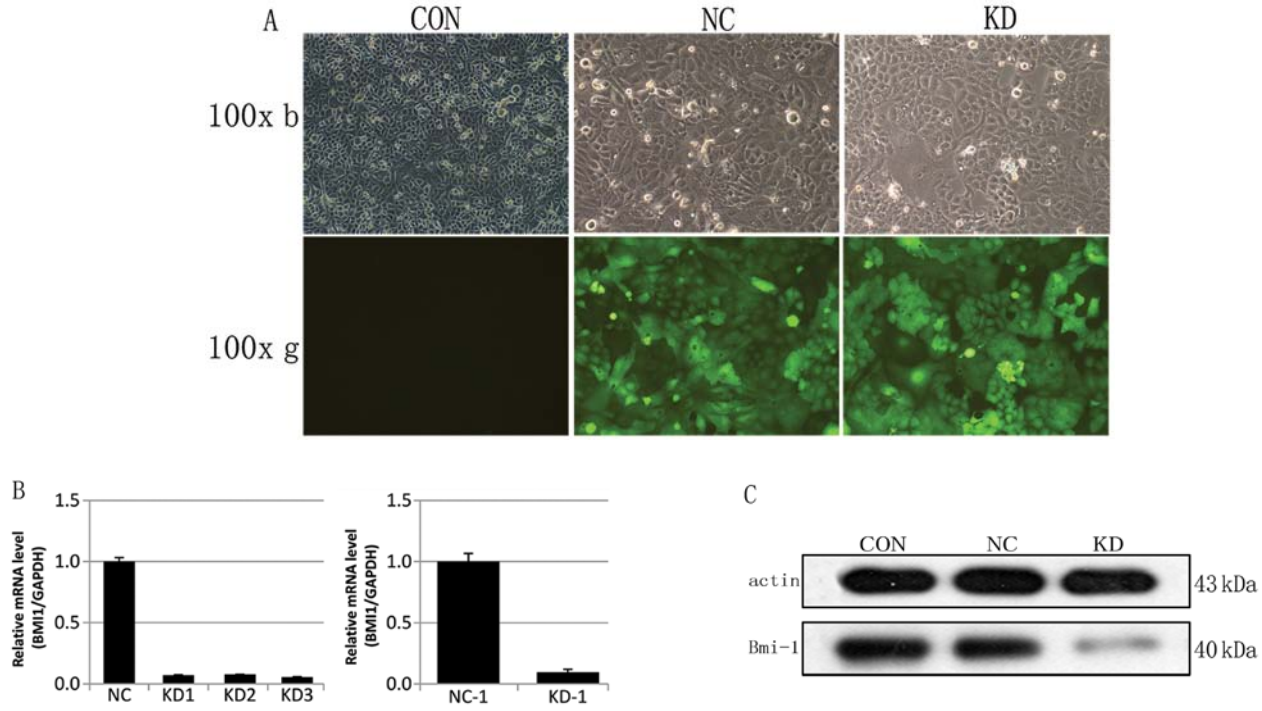

Figure 2. Lentivirus-mediated RNA targeting Bmi-1 (KD) and empty retroviral vector (NC) were constructed and transfected into CD44+ NPC cells. Untreated CD44+ NPC cells (CON) served as a control. (A) The infection efficiency was determined by fluorescent microscopy. (B) Real-time PCR verified the efficiency of silencing of Bmi-1 at 72 h after transfection and Bmi-1 gene downstream gene of p16 and p14 relative mRNA levels. (C) The expression of Bmi-1 protein was detected by western blotting 72 h after transfection. β-actin was a loading control. KD, knockdown; NC, negative control; NPC, nasopharyngeal cancer; CON, control.

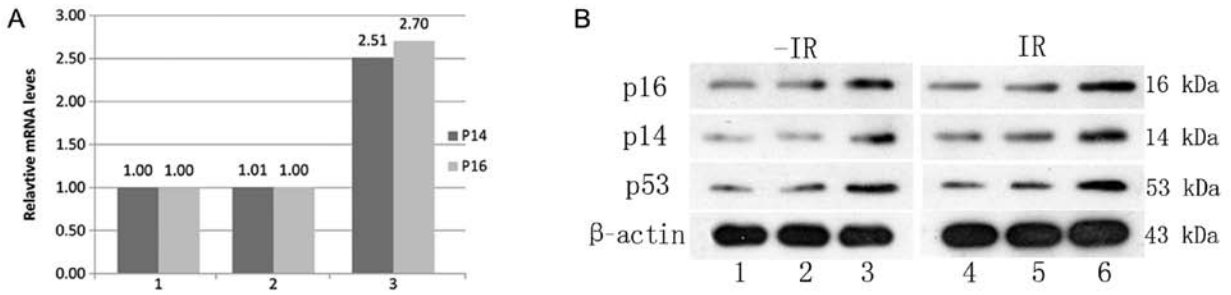

Figure 3. (A) Real-time PCR quantification of p16 and p14 mRNA expression levels in each groups. (B) Western blot analysis of Bmi-1 gene downstream related gene of p16, p14 and p53 proteins changes at 24 h following treatment with lentivirus (72 h) and subsequent 6 Gy irradiation. β-actin was a loading control. Data are displayed as one representative out of three independent experiments. Lane 1 and 4, CON; Lane 2 and 5, NC; Lane 3 and 6, KD. CON, control; NC, negative control; KD, knockdown.

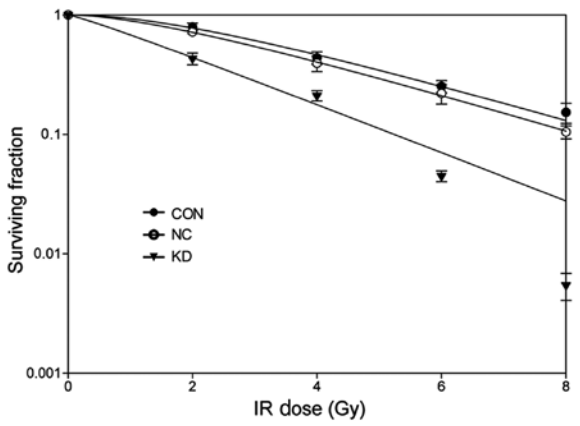

Figure 4. Downregulation of Bmi-1 increases the sensitivity of CD44+ NPC cells to irradiation. P<0.001; ANOVA test. NPC, nasopharyngeal cancer.

and the enhancement ratio was 1.77. Thus, we concluded that downregulation of Bmi-1 could radiosensitize CD44+ NPC CLCs cells.

Knockdown of Bmi-1 increases DNA double strand break (DSB) and decreases DSB repair. γH2AX is commonly utilized to assess DSBs inflicted by RT (24). When CD44+ NPC were depleted of Bmi-1, we monitored kinetics of DSB repair by immunofluorescent γH2AX foci at different time points after exposure to 2 Gy of X-rays. As shown in Fig. 5, γH2AX foci appeared immediately following IR treatment in the three groups, indicating that Bmi-1 is dispensable for γH2AX focus formation. The average number of γH2AX foci/cell in KD cells was significantly higher than in cells treated with NC or untreated/control cells at 0.5, 6, 12 and 24 h after

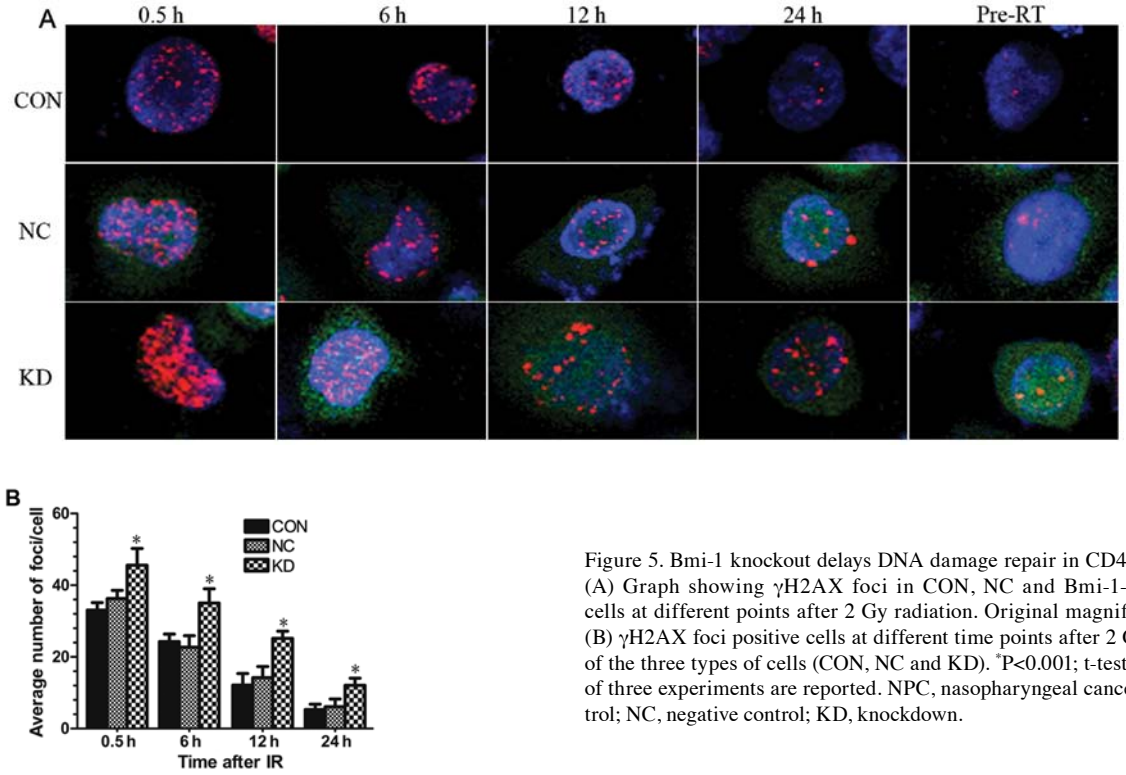

Figure 5. Bmi-1 knockout delays DNA damage repair in CD44+ NPC cells. (A) Graph showing γH2AX foci in CON, NC and Bmi-1-depleted KD cells at different points after 2 Gy radiation. Original magnification, x400. (B) γH2AX foci positive cells at different time points after 2 Gy irradiation of the three types of cells (CON, NC and KD). *P<0.001; t-test. Means ± SD of three experiments are reported. NPC, nasopharyngeal cancer; CON, control; NC, negative control; KD, knockdown.

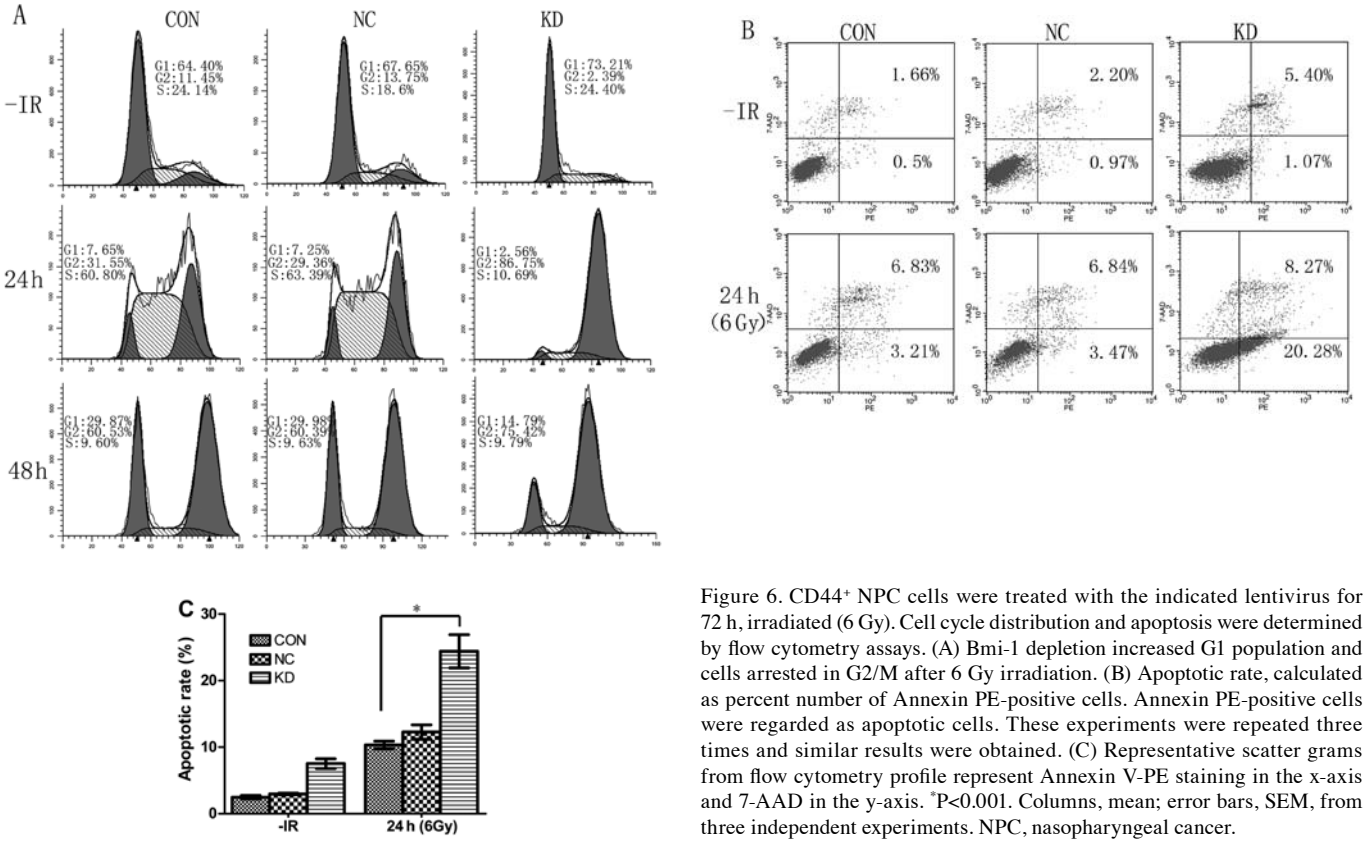

Figure 6. CD44+ NPC cells were treated with the indicated lentivirus for 72 h, irradiated (6 Gy). Cell cycle distribution and apoptosis were determined by flow cytometry assays. (A) Bmi-1 depletion increased G1 population and cells arrested in G2/M after 6 Gy irradiation. (B) Apoptotic rate, calculated as percent number of Annexin PE-positive cells. Annexin PE-positive cells were regarded as apoptotic cells. These experiments were repeated three times and similar results were obtained. (C) Representative scatter grams from flow cytometry profile represent Annexin V-PE staining in the x-axis and 7-AAD in the y-axis. *P<0.001. Columns, mean; error bars, SEM, from three independent experiments. NPC, nasopharyngeal cancer.

radiation (P<0.05). This delayed clearance of γH2AX foci in Bmi-1-depleted cells demonstrated that DSB repair is severely impaired in the absence of Bmi-1 (25).

Effects of Bmi-1 downregulation on IR-induced cell cycle distribution and apoptosis. To further evaluate potent reasons conferring radiation sensitivity induced by Bmi-1 knockdown,

we tested cell cycle distribution and cell apoptosis following treatment of lentivirus and/or IR by flow cytometry assays. As shown in Fig. 6A, compared with the blank CON group, cells treated with LV-BMI1-RNAi showed prolonged G1 from 64.40 to 73.21%. G2/M phase accumulation came to max within 24 h in the KD group after IR; however, CON and NC G2/M phase increased by 48 h after irradiation, the number of cells in G2/M in KD had to some extent decreased at 48 h after IR. The levels were still significantly greater than that for NC-treated or control cells. Depletion of Bmi-1 exhibited a markedly prolonged accumulation of cells in G2/M. In addition, there was an increase in IR-induced apoptosis in the absence of Bmi-1 (Fig. 6B). Based on these results, we concluded that knockdown of Bmi-1 leads to an extended G2/M accumulation and an increase of IR-induced apoptosis.

Discussion

Cancer stem cell theory is based on the hypothesis that cancers arise from a rare population of cells, which are responsible for the chemo- and radioresistance of the tumors. Therefore, the cancer stem cell population is thought to be an important determinant of treatment failure. Polycomb group proteins (PcG) are a family of proteins that is essential for proper embryonic development and for the specification of stem cell gene expression profiles, controlling self-renewal, pluripotency and differentiation (25), and PcG may confer radioresistance to stem cells (25). Bmi-1, a member of the Polycomb family of transcriptional repressors, is essential for maintaining the self-renewal abilities of adult stem cells. Facchino *et al* observed that Bmi-1 was responsible for the radioresistance in both glioma stem cells and normal stem cells (26). Our results demonstrate that the isolated CD44+ subpopulation from SUNE-1 5-8F human NPC cell line presents the key biological properties of CSCs and Bmi-1 was overexpressed in our previous study (16).

In the present study, we provided evidence that Bmi-1 was correlated with radiation response in CD44+ NPC CSC-LCs. We showed that Bmi-1 overexpression developed radiation resistance, whereas Bmi-1 inhibition significantly increased radiation sensitivity with a DER of 1.77 by radiation clonogenic survival assay. It suggested that Bmi-1 may play an important role in the regulation of cellular response to radiation in CD44+ NPC CSC-LCs. Thus, the results underscore the importance of Bmi-1 targeting in combination with irradiation in nasopharyngeal neoplasm therapy. This finding is consistent with the reports of Wang *et al* (13) and Alajez *et al* (15).

Bmi-1 is a transcriptional repressor of the Ink4a/Arf locus. This locus encodes 2 separate tumor suppressor genes, namely, $p16^{Ink4a}$ and $p19^{Arf}$ ($p14^{Arf}$ in humans) (27). The $p16^{INK4a}$ (pRb/p16INK4a/cyclin D1) and p53 (p14ARF/mdm2/p53) pathways are the two main cell cycle control pathways. $p16^{INK4a}$ is a potent inhibitor of the kinase activities of CDK4/6, resulting in Rb hypophosphorylation, binding to E2F1, the initiation of cell cycle arrest in the G1 phase (28). In addition, cell cycle arrest and apoptosis are promoted by p14 through its regulation of p53 stability stages, and p14 effectively prevents degradation of the tumor suppressor protein p53, which is required for cell cycle arrest. Hence, Bmi-1 knockdown inhibited cell cycle progression through derepression of the p16INK4a/p14ARF locus.

It is well known that DSBs are suggestive of critical lesions in DNA caused by ionizing radiation (29). DSB is the main mechanism of tumor cell death after irradiation (30), DNA DSB repair shows strong cell cycle dependency and radiation therapy may mediate cell cycle redistribution of tumor cells. Our findings showed that knockdown of Bmi-1 prolonged G1, after 6 Gy irritation, and the proportion of the cells in G2/M phase was increased, which was the most radiosensitive phase of the cell cycle. In addition, Gilbert *et al* showed that low-expression of p16 has been linked to decreased chemoradiotherapy responsiveness, $p16^{Ink4a}$ negative patients had significantly poorer overall survival (31). The present study showed that p16 increased after Bmi-1 inhibition and this may be one of the reasons resulting in increased DSBs and decreased DSB repair in Bmi-1 knockdown cells. Bmi-1 inhibition markedly increased DSB and significantly decreased the rate of DNA DSB repair induced by irradiation, suggesting a participation of Bmi-1 in DNA strand damage and repair (26,32). If complete DNA damage repair fails, apoptosis is triggered for the elimination of damaged cells. We noted that the number of apoptotic cells in Bmi-1 knockdown cells was apparently much higher compared with the controls using FACS analysis (Fig. 6B). The mechanism of Bmi-1 inhibition combined radiation induced apoptosis is complex. A possible reason is that the P53 pathway for apoptosis was activated in response to combined Bmi-1 inhibition with ionizing radiation (15).

In conclusion, we reported the enhanced radiosensitivity of CD44+ NPC CSCs after Bmi-1 inhibition using shRNA. The increased sensitivity was associated with increased DSBs and decreased DSB repair. We also showed that combination Bmi-1 inhibition with irradiation could induce apoptosis, elevated protein p53, p16 and p14 expression. These results suggest that Bmi-1 knockdown combined radiotherapy could induce a synergistic effect on increasing the radiosensitivity of CD44+ CSC-LCs. Bmi-1 inhibition in NPC stem cells may be an effective therapeutic strategy against NPC. However, further study is required to confirm these results using *in vivo* xenograft models.

Acknowledgements

This study was supported by The Foundation of Health Department of Hubei Province, China (no. JX4B52). We thank Jing-Hua Ren, Wei-Hong Chen, Hong-Xia Zhou and other personnel in the Laboratory of Cancer Center, the Union Hospital, the Tongji Medical College, the Huazhong University of Science and Technology (Wuhan, China) for their technical assistance.

References

1. Chargari C, Moncharmont C, Lévy A, *et al*: Cancer stem cells, cornerstone of radioresistance and perspectives for radiosensitization: glioblastoma as an example. Bull Cancer 99: 1153-1160, 2012 (In French).
2. Malik B and Nie D: Cancer stem cells and resistance to chemo and radio therapy. Front Biosci 4: 2142-2149, 2012.
3. Krause M, Yaromina A, Eicheler W, Koch U and Baumann M: Cancer stem cells: targets and potential biomarkers for radiotherapy. Clin Cancer Res 17: 7224-7229, 2011.
4. Park IK, Qian D, Kiel M, *et al*: Bmi-1 is required for maintenance of adult self-renewing haematopoietic stem cells. Nature 423: 302-305, 2003.

5. Grinstein E and Mahotka C: Stem cell divisions controlled by the proto-oncogene BMI-1. J Stem Cells 4: 141-146, 2009.
6. Lukacs RU, Memarzadeh S, Wu H and Witte ON: Bmi-1 is a crucial regulator of prostate stem cell self-renewal and malignant transformation. Cell Stem Cell 7: 682-693, 2010.
7. Yamazaki H, Mori T, Yazawa M, *et al*: Stem cell self-renewal factors Bmi1 and HMGA2 in head and neck squamous cell carcinoma: clues for diagnosis. Lab Invest 93: 1331-1338, 2013.
8. Sinha N, Mukhopadhyay S, Das DN, Panda PK and Bhutia SK: Relevance of cancer initiating/stem cells in carcinogenesis and therapy resistance in oral cancer. Oral Oncol 49: 854-862, 2013.
9. Shien K, Toyooka S, Ichimura K, *et al*: Prognostic impact of cancer stem cell-related markers in non-small cell lung cancer patients treated with induction chemoradiotherapy. Lung Cancer 77: 162-167, 2012.
10. Liu ZG, Liu L, Xu LH, *et al*: Bmi-1 induces radioresistance in MCF-7 mammary carcinoma cells. Oncol Rep 27: 1116-1122, 2012.
11. Moscatelli D and Lynette Wilson E: Bmi-1, stem cells and prostate carcinogenesis. Asian J Androl 13: 353-354, 2011.
12. Yu X, Li H, Jiang X, Guo L, Jiang W and Lu SH: miR-203 inhibits the proliferation and self-renewal of esophageal cancer stem-like cells by suppressing stem renewal factor *Bmi-1*. Stem Cells Dev 23: 576-585, 2014.
13. Wang HB, Liu GH, Zhang H, *et al*: Sp1 and c-Myc regulate transcription of *BMI1* in nasopharyngeal carcinoma. FEBS J 280: 2929-2944, 2013.
14. Wang G, Liu L, Sharma S, *et al*: Bmi-1 confers adaptive radioresistance to KYSE-150R esophageal carcinoma cells. Biochem Biophys Res Commun 425: 309-314, 2012.
15. Alajez NM, Shi W, Hui AB, *et al*: Targeted depletion of BMI1 sensitizes tumor cells to P53-mediated apoptosis in response to radiation therapy. Cell Death Differ 16: 1469-1479, 2009.
16. Su J, Xu XH, Huang Q, *et al*: Identification of cancer stem-like $CD44^+$ cells in human nasopharyngeal carcinoma cell line. Arch Med Res 42: 15-21, 2011.
17. Chen YC, Chang CJ, Hsu HS, *et al*: Inhibition of tumorigenicity and enhancement of radiochemosensitivity in head and neck squamous cell cancer-derived ALDH1-positive cells by knockdown of Bmi-1. Oral Oncol 46: 158-165, 2010.
18. Häyry V, Mäkinen LK, Atula T, *et al*: Bmi-1 expression predicts prognosis in squamous cell carcinoma of the tongue. Br J Cancer 102: 892-897, 2010.
19. Häyry V, Tynninen O, Haapasalo HK, *et al*: Stem cell protein BMI-1 is an independent marker for poor prognosis in oligodendroglial tumours. Neuropathol Appl Neurobiol 34: 555-563, 2008.
20. Smith KS, Chanda SK, Lingbeek M, *et al*: Bmi-1 regulation of INK4A-ARF is a downstream requirement for transformation of hematopoietic progenitors by E2a-Pbx1. Mol Cell 12: 393-400, 2003.
21. Calao M, Sekyere EO, Cui HJ, *et al*: Direct effects of Bmi1 on p53 protein stability inactivates oncoprotein stress responses in embryonal cancer precursor cells at tumor initiation. Oncogene 32: 3616-3626, 2013.
22. Fujii H, Honoki K, Tsujiuchi T, *et al*: Reduced expression of INK4a/ARF genes in stem-like sphere cells from rat sarcomas. Biochem Biophys Res Commun 362: 773-778, 2007.
23. Kim K, Kim DH, Chae SW, *et al*: Expression of cell cycle-related proteins, p16, p53 and p63 as important prognostic markers in gallbladder adenocarcinoma. Pathol Oncol Res 20: 409-415, 2014.
24. Scully R and Xie A: Double strand break repair functions of histone H2AX. Mutat Res 750: 5-14, 2013.
25. Gieni RS, Ismail IH, Campbell S and Hendzel MJ: Polycomb group proteins in the DNA damage response: a link between radiation resistance and 'stemness'. Cell Cycle 10: 883-894, 2011.
26. Facchino S, Abdouh M, Chatoo W and Bernier G: BMI1 confers radioresistance to normal and cancerous neural stem cells through recruitment of the DNA damage response machinery. J Neurosci 30: 10096-10111, 2010.
27. Iwama A, Oguro H, Negishi M, *et al*: Enhanced self-renewal of hematopoietic stem cells mediated by the polycomb gene product Bmi-1. Immunity 21: 843-851, 2004.
28. Huber GF, Albinger-Hegyi A, Soltermann A, *et al*: Expression patterns of Bmi-1 and p16 significantly correlate with overall, disease-specific, and recurrence-free survival in oropharyngeal squamous cell carcinoma. Cancer 117: 4659-4670, 2011.
29. Santivasi WL and Xia F: Ionizing radiation-induced DNA damage, response, and repair. Antioxid Redox Signal: Feb 3, 2014 (Epub ahead of print).
30. Mladenov E, Magin S, Soni A and Iliakis G: DNA double-strand break repair as determinant of cellular radiosensitivity to killing and target in radiation therapy. Front Oncol 3: 113, 2013.
31. Gilbert DC, Williams A, Allan K, *et al*: $p16^{INK4A}$, p53, EGFR expression and KRAS mutation status in squamous cell cancers of the anus: correlation with outcomes following chemo-radiotherapy. Radiother Oncol 109: 146-151, 2013.
32. Dong Q, Oh JE, Chen W, *et al*: Radioprotective effects of Bmi-1 involve epigenetic silencing of oxidase genes and enhanced DNA repair in normal human keratinocytes. J Invest Dermatol 131: 1216-1225, 2011.